

2

AD-A235 217



IMPLEMENTATION PAGE

Form Approved  
OMB No. 0704-0188

It is estimated to average 1 hour per response, including the time for reviewing instructions, searching existing data sources, gathering and reviewing the collection of information, sending comments regarding this burden estimate or any other aspect of this collection of information, to Washington Headquarters Service, Directorate for Information Operations and Reports, 1215 Jefferson Avenue, Suite 1204, Washington, DC 20543-0108, and to the Office of Management and Budget, Paperwork Reduction Project (0704-0188), Washington, DC 20503.

2. REPORT DATE  
April 1991

3. REPORT TYPE AND DATES COVERED  
Final Report 1 Nov 86 to 31 May 90

4. TITLE AND SUBTITLE  
STUDIES OF RESONANTLY ENHANCED MULTIPHOTON IONIZATION PROCESSES IN MOLECULES

5. FUNDING NUMBERS  
61102F 2303 B3

6. AUTHOR(S)  
VINCENT McKOY

7. PERFORMING ORGANIZATION NAME(S) AND ADDRESS(ES)  
CALIFORNIA INSTITUTE OF TECHNOLOGY  
PASADENA, CA 91125  
AFOSR-TR-

8. PERFORMING ORGANIZATION REPORT NUMBER  
91 0498

9. SPONSORING/MONITORING AGENCY NAME(S) AND ADDRESS(ES)  
AFOSR/NC  
BOLLING AFB WASHINGTON, DC 20332-6448

10. SPONSORING/MONITORING AGENCY REPORT NUMBER  
AFOSR - 87 - 0039

11. SUPPLEMENTARY NOTES

12a. DISTRIBUTION/AVAILABILITY STATEMENT  
APPROVED FOR PUBLIC RELEASE: DISTRIBUTION IS UNLIMITED

DTIC  
ELECTE  
DISTRIBUTION CODE  
MAY 08 1991  
S C D

13. ABSTRACT (Maximum 200 words)

We have completed studies of several Resonance Enhanced Multiphoton Ionization (REMPI) processes in molecules. The overall objective of this effort was to provide a robust theoretical analysis and prediction of key spectral features associated with various experimental and technology applications of this technique including its use for state-specific detection and production of species and for diagnostics in combustion and processing plasmas.

Specific achievements of this research included: (i) studies of ion vibrational distributions produced by REMPI with emphasis on anomalous behavior in these distributions in molecules and molecular fragments, e.g. OH and CF; (ii) ion rotational distributions that results from REMPI, the underlying dynamics of these processes, and the identification of schemes for enhancing state selectivity in these distributions; (iii) use of photoelectron angular distributions produced by REMPI to probe molecular alignment, an important dynamical feature in gas-surface collisions and molecular fragmentation.

14. SUBJECT TERMS  
Multiphoton ionization of molecules; theoretical studies of ion rotational and vibrational distributions; state selective production of ions.

15. NUMBER OF PAGES  
35, including cover

16. PRICE CODE

17. SECURITY CLASSIFICATION OF REPORT  
UNCLASSIFIED

18. SECURITY CLASSIFICATION OF THIS PAGE  
UNCLASSIFIED

19. SECURITY CLASSIFICATION OF ABSTRACT  
UNCLASSIFIED

20. LIMITATION OF ABSTRACT  
UL (UNLIMITED)  
SAR (SAME AS REPORT)

1503  
ALL INFORMATION CONTAINED HEREIN IS UNCLASSIFIED

# FINAL TECHNICAL REPORT

AFOSR Contract No. AFOSR-87-0039



Accession For	
NTIS GRA&I	<input checked="" type="checkbox"/>
DTIC TAB	<input type="checkbox"/>
Unannounced	<input type="checkbox"/>
Justification	
By	
Distribution/	
Availability Codes	
Dist	Avail and/or Special
A-1	

Studies of Resonantly Enhanced

Multiphoton Ionization Processes in Molecules

Performance Period: November 1, 1986 - May 31, 1990

Approved for public release;  
distribution unlimited.

91 5 06 174

## ● Overview

Resonance Enhanced Multiphoton Ionization (REMPI) utilizes laser radiation to prepare a molecule in an excited state via multiphoton absorption and to subsequently ionize that state before it can decay. A remarkable feature of REMPI is that the very narrow bandwidth of laser radiation makes this process highly *quantum-state selective* with respect to both the initial and resonant intermediate states. *The extreme state-selectivity and sensitivity make REMPI both a tool with several significant technological applications and, coupled with high-resolution and angle-resolving photoelectron spectroscopy, an important probe of the photoionization dynamics of molecular excited states at a highly state-specific level.* Some significant applications of REMPI include its use for

- (i) ultrasensitive and state-specific detection of unstable, reactive, or trace species in combustion, chemical etching, and processing plasmas,
- (ii) production of molecular ions in specific vibrational and rotational levels for use in studies of ion-molecule reactions,
- (iii) probing photofragmentation and gas-surface scattering including alignment and orientation effects in these processes,
- (iv) exploring excited state chemistry and physics at the quantum-state-specific level.

The objective of this effort was to carry out theoretical studies of these REMPI processes in molecules and molecular fragments. These studies were designed to provide a quantitatively robust analysis and prediction of key spectral features of interest in several ongoing experimental studies and applications of this technique. Specific problems of interest to us in these studies were

- **vibrational distributions of ions produced via REMPI with particular emphasis on the anomalous or non-Franck-Condon behavior of these distributions:** Such non-Franck-Condon behavior introduces serious complications both in the ex-

traction of state populations from REMPI ion signals and in the use of the technique for production of ions in specific vibrational levels. Our goal was to identify different underlying mechanisms responsible for anomalous ion vibrational distributions and to quantitatively determine these distributions in molecules and molecular fragments of interest. These mechanisms include the presence of shape<sup>1-4</sup> and autoionizing<sup>5-8</sup> resonances in the final (photoelectron continuum) state and rapid orbital evolution of the resonant Rydberg orbital with internuclear geometry.<sup>9-11</sup> Such studies can clearly provide much needed insight in designing possible REMPI schemes for producing specific vibrational distributions of ions.

● **rotational distribution of ions prepared via REMPI of specific rotational levels of resonant Rydberg states:** The generation of ions in specific rotational states offers significant opportunities in chemical reaction studies. These rotational ion distributions and their associated photoelectron angular distributions are like fingerprints of the angular momentum make-up of the photoelectron orbitals which, in turn, is determined by the torques exerted by the nonspherical potentials of molecular ions.<sup>12</sup> Through angular momentum and parity selection rules, this angular momentum coupling can be expected to lead to rotational ion distributions which cannot be accounted for on the basis of an atomic-like model of the photoionization dynamics of resonant Rydberg orbitals *including those of almost pure  $\ell$*  (ref. 13). A very promising development here has been our identification of the significant influence that Cooper minima—regions where a specific angular momentum component of the photoionization matrix element goes through zero—exert on rotational ion distributions. In fact, we have demonstrated that Cooper minima may be exploited to achieve a high degree of rotational state selectivity in molecular ion distributions. Our objective is to examine these rotational distributions quantitatively for several systems so as to gain further insight into how REMPI rotational ion distributions

can be tuned and influenced by choice of the  $\ell$ -mixing in the ionization continuum.

● **circular dichroism in photoelectron angular distributions from aligned molecules:** We have shown that photoelectron angular distributions resulting from photoionization of aligned linear molecules should exhibit a dichroic asymmetry, i.e. angular distributions from aligned states are different for photoionization with left or right circularly polarized light<sup>13</sup>. Circular dichroism is a phenomenon in which the response of a system to left and right circularly polarized light is different. Recall, furthermore, that circular dichroism is normally associated with chiral molecules i.e. molecules which have neither a plane nor center of symmetry, and not with linear molecules. Our prediction asserted that this circular dichroism in photoelectron angular distributions (CDAD)—defined as the difference between the angular distribution for photoionization by right and left circularly polarized light—arises in the electric dipole approximation (the leading term in the interaction between light and matter), occurs in linear molecules, and *would be a direct signature of the alignment of the molecule*.<sup>13</sup> A critical question that immediately arose was: would these CDAD or difference spectra be large enough to make their measurement practical and, hence, to make CDAD a useful probe of molecular alignment. Molecular alignment, which results when molecules have preferred planes of rotation, occurs in a variety of processes including surface scattering, photoabsorption, and photodissociation. A new and practical probe of alignment would clearly be desirable.

*Some important achievements of these studies* included (i) establishing that CDAD spectra of optically aligned rotational levels of the  $A^2\Sigma^+$  state of NO — a readily accessible system — should be easily measurable. In a joint experimental-theoretical study with M. G. White and his collaborators,<sup>14</sup> CDAD spectra were measured for these aligned levels of NO and seen to be of the magnitude predicted by our

calculations,<sup>14</sup> (ii) in a further collaboration with M. G. White, this CDAD technique was used for the first time to determine the spatial alignment of NO produced by UV photodissociation of methyl nitrite.<sup>15</sup> Those studies served to establish the utility of the CDAD technique for probing chemical and physical processes in which spatial alignment plays an important role; and (iii) demonstrating in a joint theoretical-experimental effort that the CDAD spectra for molecules such as NO, CO, and benzene adsorbed on substrates e.g. Pd (111) and graphite were huge.<sup>16</sup> CDAD spectra for these adsorbates reached values of up to 80% of the photoelectron spectra for unpolarized light. These studies established that the CDAD technique is a sensitive probe of adsorbate geometry and structure and photoemission dynamics.<sup>16</sup>

## ● Research Accomplishments

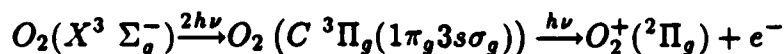
In the sections below I will review the accomplishments which have resulted from our studies of these features and applications of REMPI of molecules. A significant feature of these studies is that they were carried out using quantitatively reliable molecular photoelectron orbitals. These orbitals were taken as solutions of a one-electron Schrödinger equation containing the nonspherical potential of the molecular ion. The torques associated with these nonspherical potentials produce significant angular momentum mixing in the photoelectron orbitals. This angular momentum mixing exerts a strong influence on the dynamics of the molecular photoionization processes of interest here. For example, rotational ion distributions essentially reflect the interplay between the angular momentum of the photoelectron and that of the molecular ion.

● **Non-Franck-Condon ion vibrational distributions in REMPI of molecules and fragments:** Non-Franck-Condon behavior in the vibrational distribution of ions produced by REMPI introduces serious complications into such important applications of the technique as its use for state-specific production of ions and for the determination

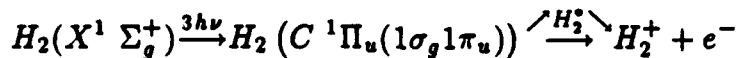
of state populations from ion signals. For example, the resonant level in many REMPI schemes is often chosen to be a molecular Rydberg state. Photoionization of these Rydberg states is generally expected to occur with preservation of vibrational quantum number.<sup>17</sup> For Rydberg levels which are well described by a single, highly excited electron with a specific ionic core, the near-identity of the neutral and ionic potential surfaces leads to Franck-Condon ion distributions, specifically  $\Delta v = v^+ - v' = 0$ . Here  $v'$  and  $v^+$  are the vibrational quantum numbers for the neutral Rydberg state and the ion respectively.

We have studied non-Franck-Condon behavior in ion vibrational distributions arising from three different mechanisms. These mechanisms, along with the specific examples chosen to illustrate the mechanism and magnitude of these effects, are

- (a) shape (one-electron) resonances in the ionization continuum, e.g.,

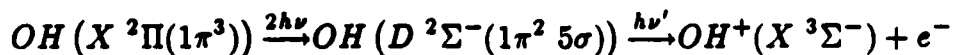


- (b) electronic autoionization of doubly excited states, e.g.,



where we schematically illustrate the presence of direct and indirect ( $H_2^*$ ) ionization channels.

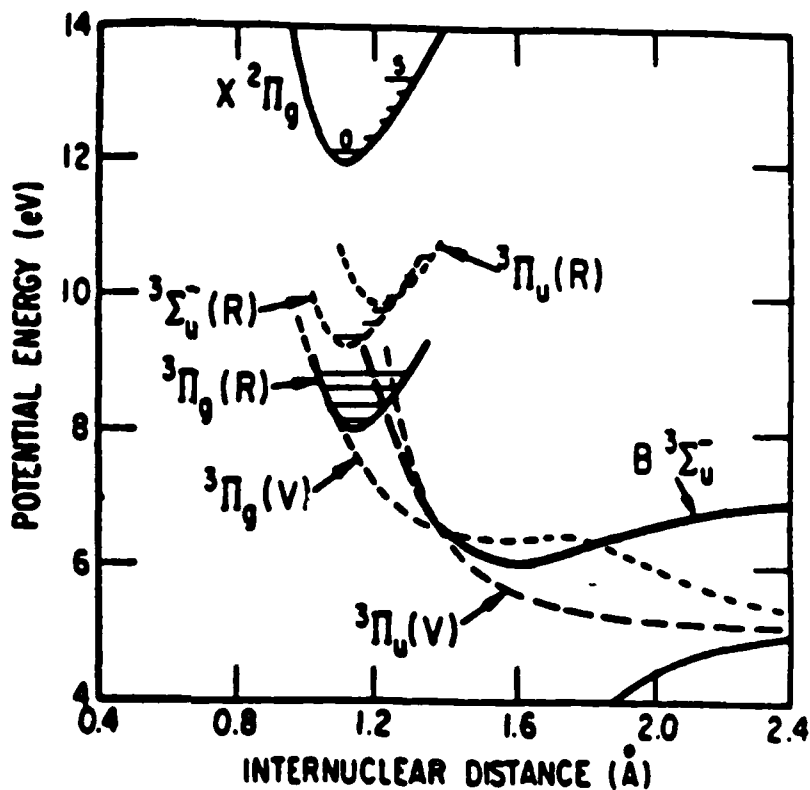
- (c) Rydberg orbitals which evolve rapidly with internuclear distance, e.g.,



*The results of these studies are as follows:*

(a) *Shape resonances in the ionization continuum:* Recent measurements of the vibrationally resolved (2+1)-REMPI spectra of  $O_2$  via the  $C^3 \Pi_g(1\pi_g 3s\sigma_g)$  Rydberg state showed non-Franck-Condon ionic state distributions, evident in the observation of intense

- The situation in (2 + 1)-REMPI of  $O_2$  via the  $C^3\Pi_g(1\pi_g3s\sigma_g)$  state. Note the curve marked  $^3\Pi_u(V)$  with outer electron configuration  $1\pi_g3\sigma_u$ .

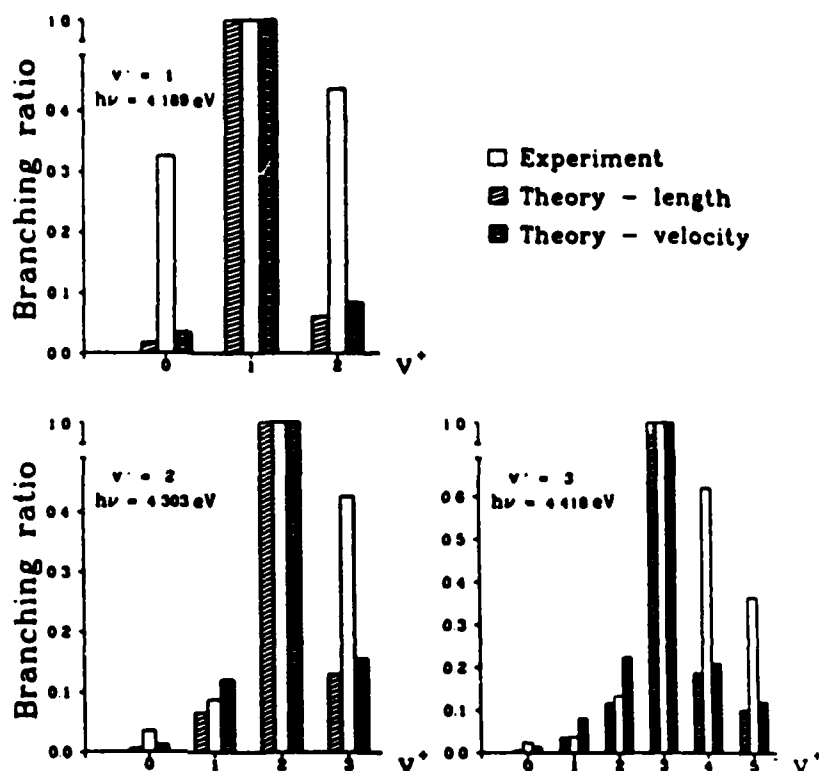


off-diagonal peaks ( $\Delta v = v' - v^+ \neq 0$ ).<sup>18</sup> This was in strong contrast to the “clean” production of  $O_2^+$  in a specific  $v^+$  level that could be expected from this scheme on the basis of Franck-Condon behavior. We have carried out *ab initio* calculations of these vibrationally resolved photoelectron spectra of the  $C^3\Pi_g$  state which have been measured by Miller et al.<sup>18</sup> These calculations establish that in the photoionization of this resonantly prepared Rydberg state a shape resonance near threshold significantly alters vibrational distributions from those based on the Franck-Condon principle.<sup>1</sup> This shape resonance and its effect on ionic vibrational branching ratios are well known from single-photon studies of first-row diatomic molecules.<sup>19</sup> Such shape resonances or quasibound states make the photoionization matrix element strongly dependent on internuclear distance and hence lead to a breakdown of the Franck-Condon principle.<sup>19</sup> Here the shape resonance is essentially a “continuation into the continuum” of the  $3\sigma_u$  orbital associated with the valence-like  $^3\Pi_u(V)$  state at larger internuclear distances (see insert above).

In the next insert we show our calculated branching ratios for REMPI via the  $v' = 1 - 3$  levels along with the relative peak intensities from the measurements of Miller



- Vibrational branching ratios for  $(2 + 1)$ -REMPI via the  $C^3\Pi_g$  ( $v' = 1 - 3$ ) state of  $O_2$ . The calculated results were normalized to the experimental data of Chupka and coworkers (*J. Chem. Phys.* **89**, 3921 (1988)) by dividing by the  $\Delta v = 0$  peak.

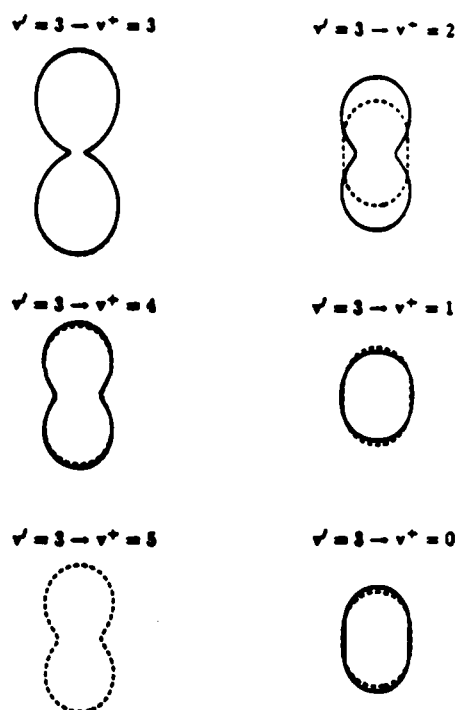


et al.<sup>18</sup> The calculations show pronounced non-Franck-Condon distributions. Note that the *Franck-Condon factors are negligible when plotted on the scale of this figure*. Discrepancies remain between the calculated and measured branching ratios in some portions of the spectra. For the  $v' = 2$  and 3 levels, the  $\Delta v < 0$  ratios agree quite well with experiment, while those for  $\Delta v > 0$  show systematic deviations. There is also substantial disagreement in these branching ratios for  $v' = 1$ . These discrepancies are almost certainly due to the presence of autoionizing states such as the  $^3\Delta_u$ ,  $^3\Sigma_u^+$ , and  $B^3\Sigma_u^-$  states arising from the  $3\sigma_g^2 1\pi_u^3 1\pi_g^3$  electron configuration and others.<sup>1</sup> Although these valence-shell excitations are not dipole-accessible from the  $C^3\Pi_g$  ( $1\pi_g 3s\sigma_g$ ) state, they couple to the direct continuum ( $1\pi_g k\pi_u$ ) via electron correlation and can hence influence the photoionization matrix element. Calculations including the effects of these autoionizing states on the ion vibrational distributions in the REMPI spectra of  $O_2$  are under way. As we will see again below, *REMPI via higher  $v'$  levels shows considerable promise as a unique and precise probe of such doubly excited autoionizing states at larger internuclear distances and*

*near-threshold energies.* Such states play an important role in dissociative recombination processes, e.g.,  $e^- + O_2^+ \rightarrow O_2^* \rightarrow 2O$ . Most available experimental data on the potential energy curves of these doubly excited states is in the Franck-Condon region of the ground state and hence on the strongly repulsive parts of their potential curves.

We have also determined the photoelectron angular distributions for these REMPI spectra of the  $C^3\Pi_g$  state of  $O_2$  (ref. 3). The photoelectron angular distributions show a substantial dependence on vibrational level and agree quite well with the measurements of Miller et al.<sup>20</sup> (see insert).

- Vibrational state dependence of photoelectron angular distributions for (2 + 1)-REMPI via the  $v' = 3$  level of the  $C^3\Pi_g$  state of  $O_2$ : —, calculated results; —, experimental data of P. J. Miller, W. A. Chupka, J. Winniczek, and M. G. White, *J. Chem. Phys.* **89**, 4058 (1988).

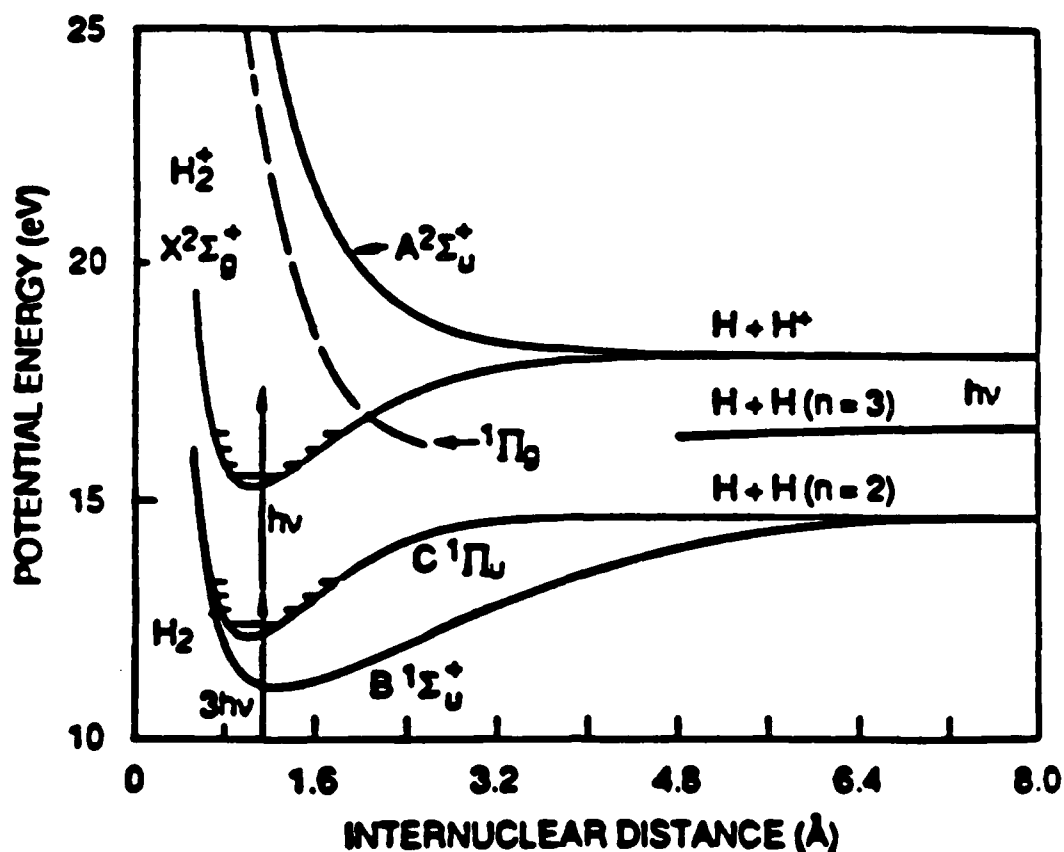


In addition to these studies of the vibrational distributions of  $O_2^+$  obtained by REMPI via the  $C^3\Pi_g$  state we have carried out similar calculations for the  $d^1\Pi_g$  ( $1\pi_g 3s\sigma_g$ ) state. The ion signals for (2 + 1)-REMPI through this state are of the order of 10% of those for the  $C^3\Pi_g$  (ref. 21). The  $\sigma_u$  shape resonance again leads to significant non-Franck-Condon ion vibrational distributions but *this now occurs at higher photoelectron energies*. This simply reflects the splitting between the  $^1\Pi_u$  ( $1\pi_g k\sigma_u$ ) and  $^3\Pi_u$  ( $1\pi_g k\sigma_u$ ) multiplets associated with the shape resonance for photoionization via the  $^1\Pi_g$  ( $1\pi_g 3s\sigma_g$ ) and  $^3\Pi_g$  ( $1\pi_g 3s\sigma_g$ ) states, respectively. This is analogous to singlet-triplet splittings seen

in absorption spectra.

(b) *Autoionization of doubly excited states*: In some early and very seminal experimental studies, Pratt et al.<sup>22</sup> measured the vibrational branching ratios resulting from (3+1)-REMPI of  $H_2$  via the  $C\ ^1\Pi_u$  state. Due to the Rydberg nature of the  $C\ ^1\Pi_u$  ( $1\sigma_g 1\pi_u$ ) state, the potential energy curves of the  $C$  state and the ground state ( $X^2\Sigma_g^+$ ) of  $H_2^+$  are nearly identical and one again expects ionization to preserve the vibrational quantum number ( $v'$ ) of the resonant state. This expected Franck-Condon behavior clearly suggests schemes for state-specific production of highly excited  $H_2^+$ . The photoelectron spectra measured along the laser polarization axis showed significant non-Franck-Condon behavior with  $\Delta v \neq 0$  peaks of increasing intensities for excitation through higher vibrational levels ( $v' > 2$ ) of the  $C\ ^1\Pi_u$  state.<sup>22</sup> In a first attempt to understand the physical origin of this non-Franck-Condon behavior we determined branching ratios including the dependence of the photoionization matrix element on photoelectron kinetic energy and internuclear distance.<sup>23</sup> While the calculated and measured branching ratios agreed well for ionization via the  $v' \neq 0 - 2$  levels, significant discrepancies remained for  $v' > 2$ .

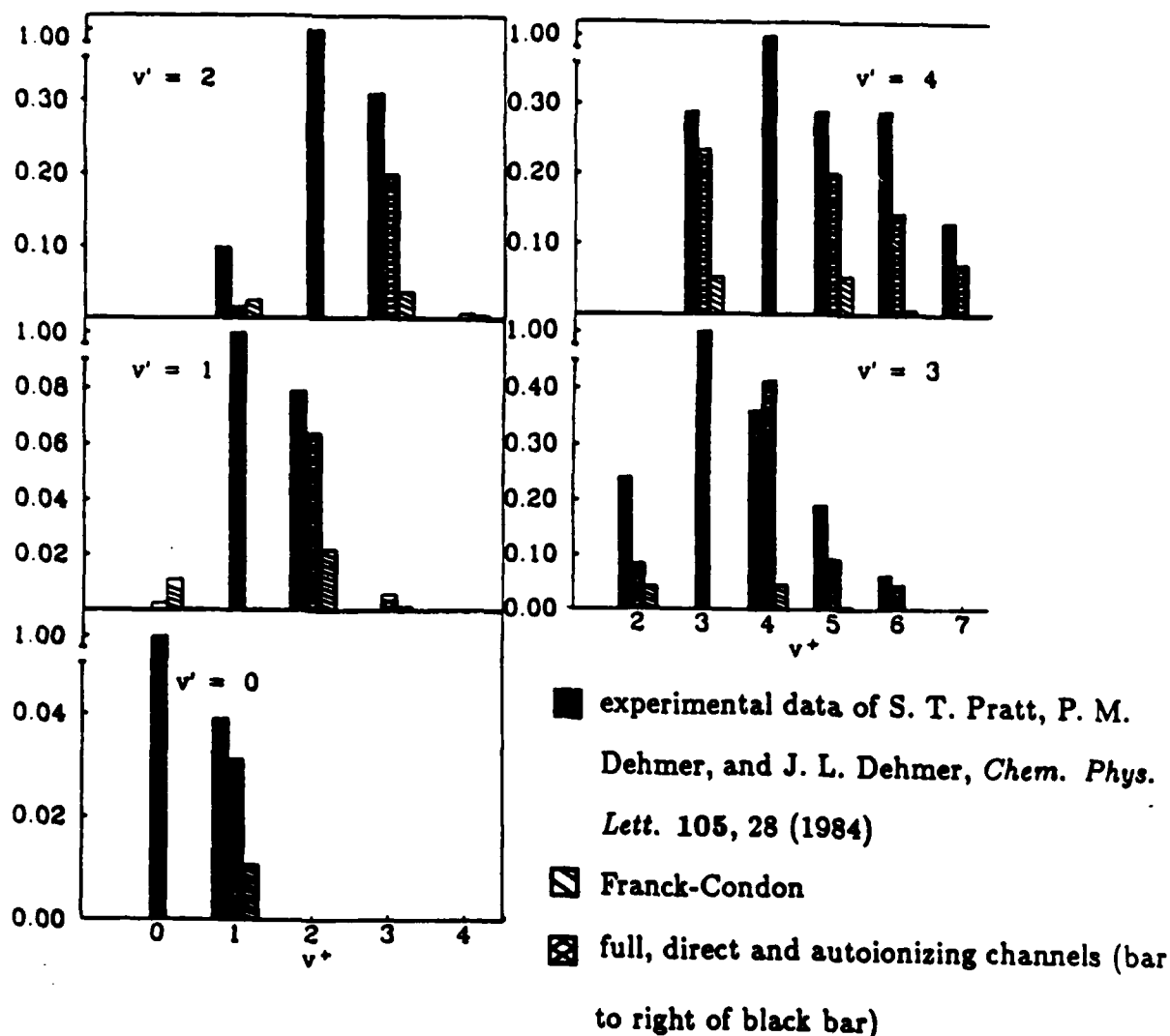
Chupka<sup>7</sup> and Hickman<sup>8</sup> had previously proposed that these anomalous ion vibrational distributions for REMPI through the  $v' > 2$  levels of the  $C\ ^1\Pi_u$  state arise from electronic autoionization via the doubly excited  $^1\Pi_g$  ( $1\sigma_u 1\pi_u$ ) state (see insert). Autoionization through these doubly excited states introduces an indirect contribution to the ionization process which interferes with the direct amplitude. We have completed *ab initio* calculations of the vibrational branching ratios for this (3 + 1)-REMPI of  $H_2$  via different vibrational levels of the  $C\ ^1\Pi_u$  state of  $H_2$  incorporating both the direct and indirect channel ( $^1\Pi_g$  state) (ref. 5). Our calculated branching ratios are compared with the measured values of ref. 22 in the insert. The agreement between these branching ratios is encouraging. These studies show that the direct and indirect amplitudes are comparable for ionization via the higher  $v' (\geq 2)$  levels. Model calculations of these vibrational ion distributions by Hickman only included a contribution from the indirect (autoionizing) channel.<sup>8</sup>



- Doubly excited autoionizing  $^1\Pi_g$  ( $1\sigma_u 1\pi_u$ ) state perturbing the vibrational distribution in REMPI of  $H_2$  via the  $C^1\Pi_u$  state. Recall that this  $^1\Pi_g$  state has a finite width (not shown).

These results represent the *first ab initio studies of the role of autoionizing states on ion vibrational distributions in REMPI of molecules*. Such dissociative autoionizing states can be expected to perturb the ion vibrational spectra produced by REMPI. *The presence of autoionization obviously introduces serious complications in the use of REMPI for the determination of state populations and for the production of state-specific ( $v^+$ ) ions*. Studies of the type we have discussed here for  $H_2$  are needed in understanding and designing such applications of REMPI. On the other hand REMPI via high vibrational levels of the resonant state can become a major probe of these doubly excited states at large internuclear distances where very little is known experimentally about their potential energy curves.

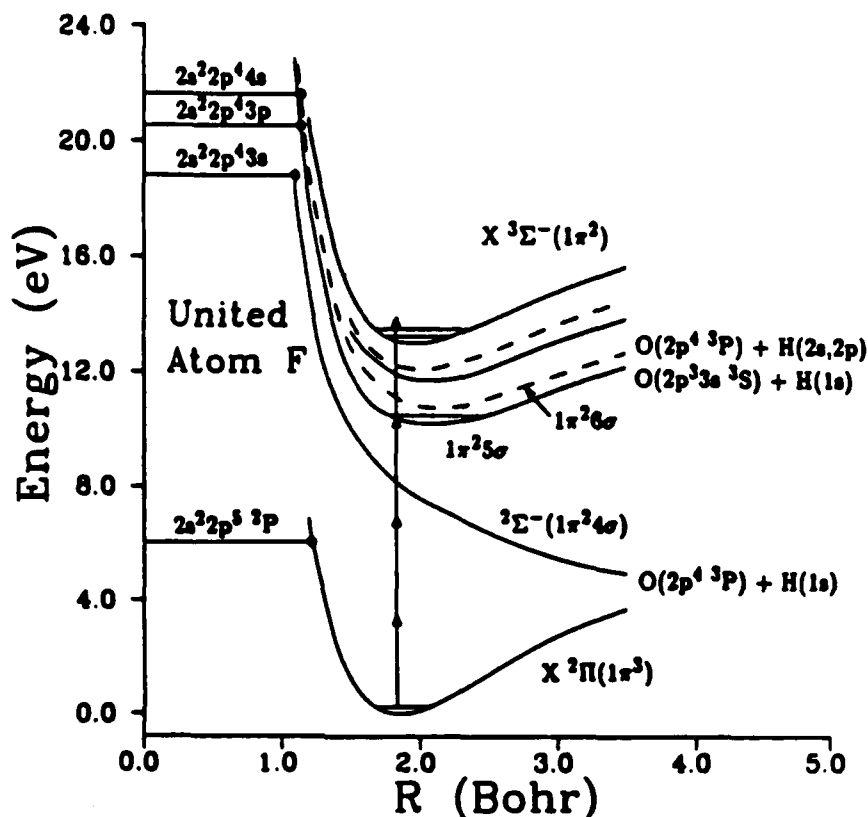
(c) *Rydberg orbital evolution*: The non-Franck-Condon behavior of ion vibrational distributions seen in the examples we have discussed above arose from electronic autoion-



- Vibrational branching ratios in (3 + 1)-REMPI of H<sub>2</sub> via the C <sup>1</sup>Π<sub>u</sub> state. ν' denotes the vibrational level of the C <sup>1</sup>Π<sub>u</sub> state and ν<sup>+</sup> that of the ion.

ization of dissociative autoionizing excited states and shape resonances in the ionization continuum. These effects derive from considerations of final-state photoionization dynamics. We also predicted a new mechanism for producing very significant non-Franck-Condon vibrational distributions which *derives solely from a property of the Rydberg orbital of the resonant state*. This property is that the Rydberg orbital should evolve rather rapidly into its united or separated atom limits over a range of internuclear distance associated with low vibrational levels. *Molecular Rydberg orbitals with these characteristics typically occur in diatomic hydrides, e.g., OH, CH, NH, an important class of species in multiphoton*

- Potential energy curves for  $OH$ . REMPI is via the  $^2\Sigma^-(1\pi^25\sigma)$  state. The character of the  $5\sigma$  orbital evolves from primarily  $3p$  at small  $R$  to  $3s$  at large  $R$ .



ionization photodissociation and photofragmentation problems.

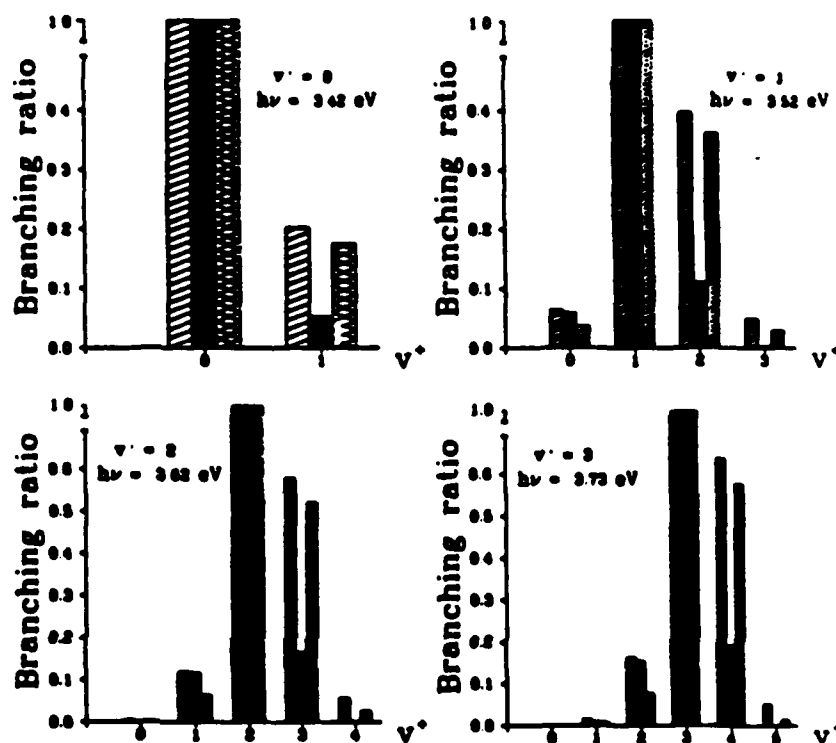
We quantitatively examined this mechanism with specific predictions of ion vibrational distributions for a proposed  $(3 + 1)$ -one-color measurement of  $OH$  via the  $D^2\Sigma^-(1\pi^25\sigma)$  state. In the insert we show potential energy curves for the  $X^2\Pi(1\pi^3)$  ground state of  $OH$ , the  $X^3\Sigma^-(1\pi^2)$  state of  $OH^+$ , and several excited state curves with outer electronic configurations  $^2\Sigma^-(1\pi^2n\sigma)$  for  $n = 4 - 8$ . The repulsive nature of the  $^2\Sigma^-(1\pi^24\sigma)$  state arises from "Rydbergization" of an antibonding  $2p_O - 1s_H$  molecular orbital into the fluorine  $3s$  orbital at small  $R$  (ref. 24). The  $5\sigma$  orbital of the  $^2\Sigma^-(1\pi^25\sigma)$  state correlates with a  $3p$  atomic orbital at small  $R$  and a  $3s$  at large  $R$ . The angular momentum composition of this orbital varies rapidly as the internuclear distance changes.<sup>9</sup> Accompanying this rapid variation in angular momentum composition are changes in the

nodal structure of the excited-state wavefunction. The principal result of this behavior is that the electronic transition moment is a strong function of internuclear distance and hence the usual Franck-Condon factorization becomes invalid. We can hence expect significant departures from the  $\Delta v = 0$  propensity rule for producing molecular ions in different vibrational states. Our calculated branching ratios for photoionization of the  $v' = 0 - 3$  levels of the  $^2\Sigma^- (1\pi^25\sigma)$  Rydberg state, shown in the insert, substantiate this prediction. The Franck-Condon branching ratios are at most about 0.2. With inclusion of the  $R$ -dependence of the photoionization matrix elements, we find very large deviations from these Franck-Condon predictions. For the  $\Delta v = 1$  branching ratios the enhancement over the Franck-Condon results is typically about 3. For the  $\Delta v = 2$  transitions, the enhancements are much larger.

In summary, we identified a new mechanism by which molecular ion vibrational distributions produced in REMPI experiments can deviate substantially from the well-known  $\Delta v = 0$  propensity rule. Measurements of these branching ratios in REMPI of  $OH$  are under consideration by one or two experimental groups. A significant implication of these studies is that *this effect is not restricted to  $OH$  but will generally be pronounced in diatomic hydrides since their electronic structure is close to the corresponding united atom.*

● *Rotational distributions of molecular ions produced via REMPI:* REMPI offers wide possibilities for producing molecular ions in specific rotational levels via photoionization of a selected rotational level of the excited resonant state. Coupled with energy- and angle-resolved photoelectron spectroscopy, rotationally resolved REMPI also clearly provides a significant window on the photoionization dynamics of excited states. Whereas ionic rotational levels have been resolved in the photoelectron spectra of  $H_2$  with its large rotational spacing quite easily, rotational resolution has been difficult for heavier ions because of their smaller rotational constants. However, Reilly and coworkers<sup>25,26</sup> recently obtained rotationally resolved spectra in REMPI of  $NO$  via high  $J$  levels of the  $A^2\Sigma^+$

- Calculated vibrational branching ratios for (3 + 1) REMPI of *OH* via the  $D\ ^2\Sigma^-$  ( $v' = 0 - 3$ ) state. The one-photon energies are shown in each frame. The solid central bar shows the Franck-Condon ratio. The calculated non-Franck-Condon branching ratios are shown to the left (length form) and right (velocity form) of the Franck-Condon values. This behavior is expected in other hydrides such as *CH* and *NH*.



and  $D\ ^2\Sigma^+$  states. Zare and his collaborators<sup>27</sup> have determined photoelectron distributions for these rotationally resolved spectra in two-color REMPI through the  $A\ ^2\Sigma^+$  state of *NO*. Furthermore, Schlag and coworkers<sup>28</sup> have developed a novel method of zero-kinetic-energy (ZEKE) photoelectron spectroscopy which provides total (no angular resolution) rotationally resolved cross sections with a resolution of 1-2  $\text{cm}^{-1}$ . This technique can provide rotationally resolved ion spectra for low rotational levels. With such high-resolution techniques available in laser photoelectron spectroscopy, one can expect an upsurge in experimental studies of rotationally resolved ion spectra of diatomic and small polyatomic molecules.

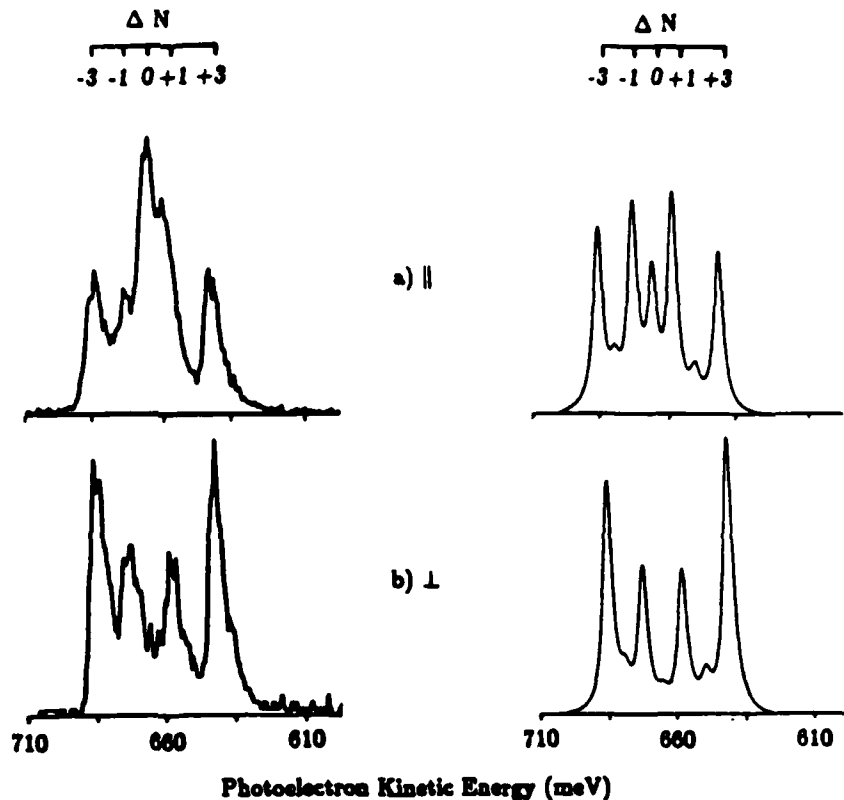


We have completed several studies of the rotationally resolved REMPI photoelectron spectra of  $NO$  via the  $D^2\Sigma^+ (3p\sigma)$  and the  $A^2\Sigma^+ (3s\sigma)$  states, processes for which recent experimental data reveal several dynamically significant features.<sup>25-28</sup> Some highlights of these studies were as follows.

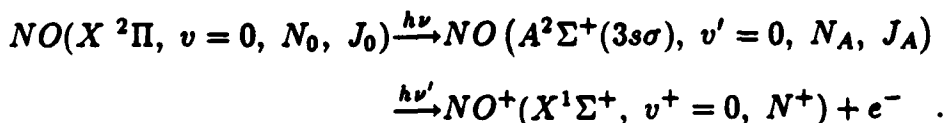
(a) the measured rotational branching ratios for (2+1)-REMPI via the  $D^2\Sigma^+ (3p\sigma)$  state of  $NO$  show a very strong  $\Delta N = 0$  peak for photoelectron detection parallel to the laser polarization.<sup>26</sup> Here  $\Delta N$  is the change in angular momentum quantum numbers, exclusive of spin, between the resonant and ionic states. A selection rule governing the possible values of angular momentum transfer,  $\Delta N$ , and  $\ell$ , an angular momentum component of the photoelectron orbital, for such a  $\Sigma^+ \rightarrow \Sigma^+$  transition, ( $\Delta N + \ell = \text{odd}$ ), establishes that this  $\Delta N = 0$  peak must arise from a  $3p \rightarrow kp$  ionizing transition.<sup>29</sup> Such  $p \rightarrow p$  transitions are forbidden in any atomic-like model. In fact, photoionization of this resonant orbital would be expected to occur via  $3p \rightarrow ks$  and  $kd$  transitions and should hence lead to odd  $\Delta N$  peaks in the rotational spectrum ( $\Delta N = \text{odd}$  for  $\ell = 0$  and 2). Our calculated branching ratios (see following insert) do show a significant  $\Delta N = 0$  peak which can be explicitly shown to be due to the substantial  $p$ -wave component of the photoelectron wave function<sup>12,30</sup> This  $p$ -wave character arises, in turn, from  $\ell$ -mixing in the photoelectron wave function caused by the nonspherical potential of the molecular ion. This is purely a molecular effect and clearly *illustrates the role the anisotropy of the molecular ion potential plays in determining rotational distributions*. The  $p$ -wave character of the photoelectron's wavefunction associated with the  $\Delta N = 0$  peaks in this spectrum is further supported by their absence for photoelectron detection perpendicular to the laser polarization, i.e., a  $\cos^2\theta$  behavior.

(b) the rotational resolution in the experiments discussed above<sup>26</sup> could be achieved by accessing high rotational levels. With its photoelectron energy resolution of about  $1 \text{ cm}^{-1}$ , ZEKE-photoelectron spectroscopy has been used by Schlag and coworkers<sup>28</sup> to

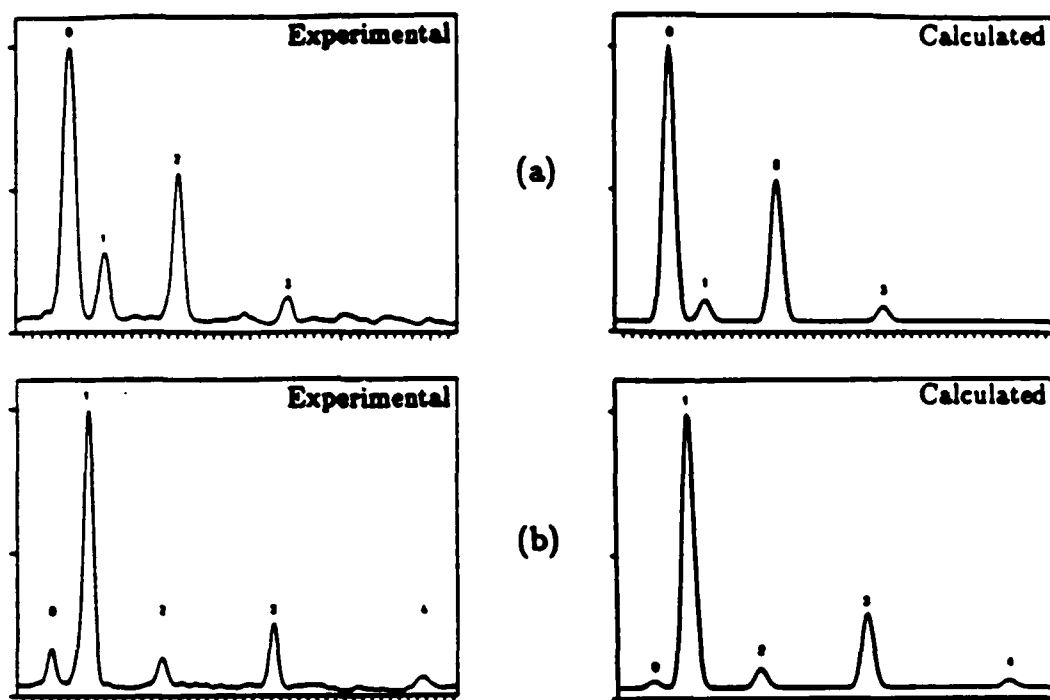
- Calculated (right) and measured (left) rotationally resolved photoelectron spectra for (2 + 1)-REMPI of *NO* via the  $S_{21}$  (11.5) line of the  $X^2\Pi \rightarrow D^2\Sigma^+$  transition: (a), photoelectron detection parallel to laser polarization; (b), photoelectron detection perpendicular to laser polarization. The experimental data is taken from ref. 26.



determine rotational branching ratios for (1 + 1')-REMPI of *NO* via low rotational levels ( $N_A = 0, 1, 2, 3$ ) of the  $A^2\Sigma^+$  state, i.e.,



The selection rule  $\Delta N + \ell = \text{odd}$  predicts that even  $\Delta N$  peaks should be dominant in the photoelectron spectrum of this  $3s\sigma$  ( $\ell_0 = 0$ ) orbital with its 94% *s*-character, i.e.,  $\ell_0 = 0 \rightarrow \ell = 1$ , makes  $\Delta N$  even.<sup>29</sup> However, appreciable odd  $\Delta N$  peaks are also seen in the spectrum.<sup>28</sup> These peaks reflect the presence of even waves in the photoelectron wave functions due to angular momentum coupling by the molecular potential. Such spectral features are in general agreement with earlier studies of REMPI of *NO* via higher *N* levels of the  $A^2\Sigma^+$  state.<sup>25,31</sup> However, an additional striking feature of these spectra



- (a) Experimental (ref. 28) and our calculated photoelectron spectra for REMPI via the  $P_{11}(3/2)$  branch of the  $0-0$  band of the  $X^2\Pi - A^2\Sigma^+$  transition ( $J_A = 1/2$ ,  $N_A = 0$ ). The value of  $N_A$  is shown above each peak; (b) same as (a) but via the  $P_{11}(5/2)$  branch,  $J_A = 3/2$ ,  $N_A = 1$ .

was the strong dependence of this angular momentum transfer  $\Delta N$  on the value of  $N$  in the resonant state.<sup>35</sup> Explicit calculations at very low photoelectron energy<sup>32</sup> reproduce the strong decrease in the ratio of the  $\Delta N = 0$  to  $\Delta N = +2$  peaks seen experimentally when  $J_A$  increases from  $\frac{1}{2}$  to  $\frac{3}{2}$  (see insert above) but do not show the rapid die-off of the  $\Delta N \neq 0$  peaks for higher  $J_A$  levels observed in the experiments of Schlag's group.<sup>28</sup> This trend in the  $\Delta N = 0$  to  $\Delta N = 2$  peak ratios for  $N_A = \frac{1}{2}$  and  $\frac{3}{2}$  has been shown to be due to simple angular momentum transfer arguments.<sup>32</sup> These arguments also predicted that this trend in  $\Delta N = 0$  to 2 peak intensities observed for this specific branch ( $P_{11}$ ) with increasing angular momentum in the resonant state should not be generally expected in other branches.<sup>32</sup>

- (c) Combined with photoelectron angular detection, rotationally resolved spectra

can be expected to provide an even more detailed dynamical picture of molecular photoionization. For example, photoelectron angular measurements parallel and perpendicular to the polarization vector of the light by Reilly and coworkers<sup>26</sup> in rotationally resolved REMPI via the  $D^2\Sigma^+$  ( $3p\sigma$ ) state of  $NO$  made it possible to explicitly identify the surprisingly large  $p$ -wave character of the photoelectron wave function. Two significant dynamical features of the spectra that can be probed by such measurements are the dependence of the photoelectron angular distributions on the rotational state of the ion and on the alignment of the resonantly prepared state.<sup>33</sup> These angular distributions are a specific probe of the angular momentum composition of the photoelectron orbital.

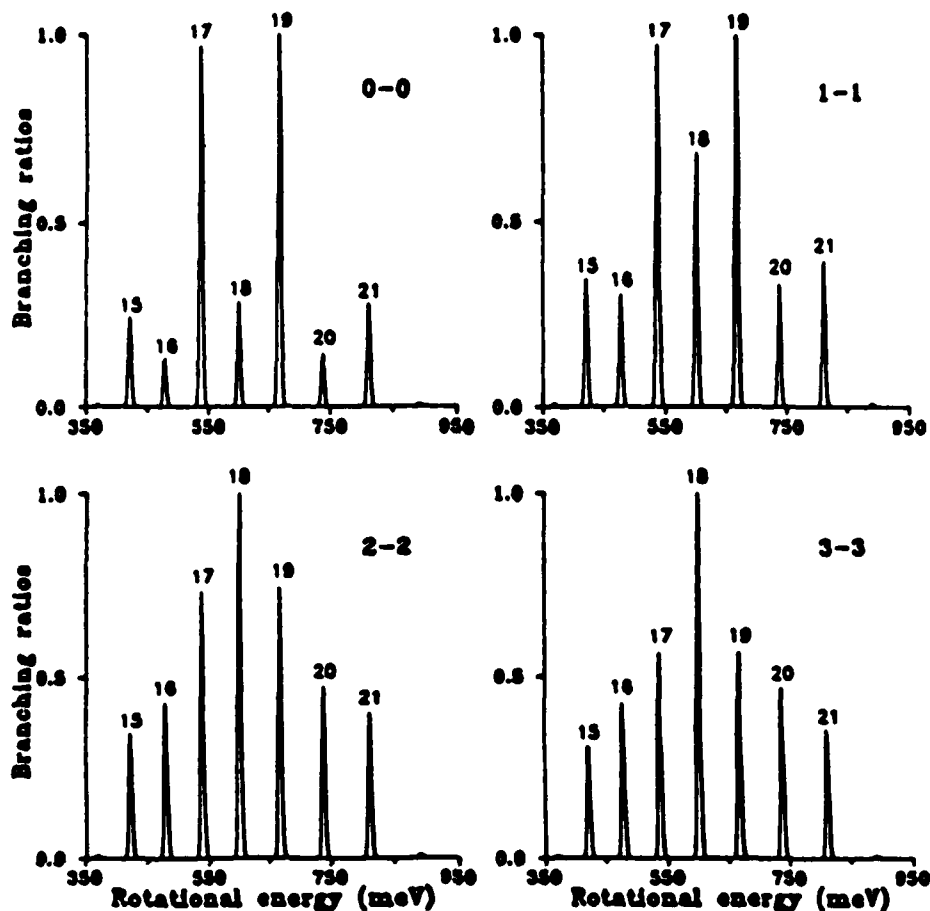
We completed studies of the photoelectron angular distributions for rotationally resolved spectra arising from two-color  $(1+1')$ -REMPI via the  $R_{21}$  (20.5),  $P_{21} + Q_{11}$  (25.5) and  $P_{11}$  (22.5) branches of the  $A^2\Sigma^+$  ( $3s\sigma$ ) state of  $NO$  (ref. 33). The insert below compares our calculated photoelectron angular distributions for the mixed  $P_{21} + Q_{11}$  (25.5) branch with the very recent measurements of Allendorf et al.<sup>27</sup> While the  $\Delta N = 0$  peaks, which account for nearly 80% of the photoelectron flux, are dominated by  $p$ -wave character, the  $\Delta N = \mp 2$  peaks exhibit far more  $f$ -wave character with a smaller contribution from  $p$ -waves. These results showed that when the rotational state of the ion is not resolved, the loss of information is striking. Differences in the calculated photoelectron angular distributions for the  $P_{21} + Q_{11}$  (25.5) and  $P_{11}$  (22.5) branches also reveal the sensitivity of these distributions to intermediate state alignment. Together these results illustrate the dynamical richness of rotationally resolved REMPI photoelectron spectra.

In our earlier discussion we showed that rapid evolution of the angular momentum composition of a resonant Rydberg orbital can be expected to lead to significantly non-Franck-Condon behavior in ion vibrational distributions.<sup>9</sup> This effect was illustrated with specific predictions for REMPI of  $OH$  (ref. 9). We also showed that such orbital evolution has a striking and significant influence on ionic rotational distributions as the level of vibrational excitation in the resonant Rydberg orbital increases.<sup>34</sup> As an example of this

	$\Delta N$					unres.
	-2	-1	0	+1	+2	
$P_{21}+Q_{11}(25.5)$ experimental						
$P_{21}+Q_{11}(25.5)$ calculated						
$P_{11}(22.5)$ calculated						

- Calculated (ref. 33) and measured (ref. 27) rotationally resolved ( $\Delta N = -2, -1, 0, +1, +2$ ) photoelectron angular distributions for  $(1+1')$  REMPI via the  $P_{21} + Q_{11}$  (25.5) branch of the  $A \ ^2\Sigma^+(3s\sigma)$  state of  $NO$ . Calculated distributions for the pure  $P_{11}(22.5)$  branch.

effect we examined two-color  $(2 + 1')$ -REMPI of  $CH$  via the  $E' \ ^2\Sigma^+ (3p\sigma)$  state. The dominant electron configuration of this state is  $1\sigma^2 2\sigma^2 3\sigma^2 5\sigma$ . As in the case of  $OH$  the  $5\sigma$  orbital evolves rapidly from predominantly  $3p$  character at small internuclear distances to predominantly  $3s$  character at larger distances. This orbital evolution results in a dramatic dependence of the partial wave composition of the photoelectron transition moment on internuclear distance. An atomic picture of this process would predict even partial waves, i.e.,  $3p \rightarrow ks, kd$ , to be dominant at small  $R$  and odd partial waves, i.e.,  $3s \rightarrow kp$ , to be dominant at larger internuclear distances. For the  $\Sigma \rightarrow \Sigma$  photoionizing transition here



- Illustration of the dependence of ionic rotational branching ratios on vibrational level of the resonant Rydberg state accessed. These results are for  $(2 + 1')$  REMPI via the  $O_{11}(20.5)$  branch of the  $E' \ ^2\Sigma^+(3p\sigma)$  state of  $CH$  for various vibrational levels. The values of  $v_i$  and  $v_+$  are shown in the upper right corner of each frame. The value of  $N_+$  is indicated over each photoelectron peak.

a  $\Delta N + \ell = \text{odd}$  selection rule applies, where  $\Delta N$  is the change in the rotational quantum number (exclusive of spin) between the intermediate and final state and  $\ell$  denotes an angular momentum component of the photoelectron orbital. This selection rule suggests that at smaller internuclear distances odd  $\Delta N$  transitions are favored while even  $\Delta N$  transitions should be favored at larger distances.

The insert below shows predicted ionic rotational branching ratios for the  $O_{11} (20.5)$  branch via the  $E' \ ^2\Sigma^+$  state of  $CH$  for the  $v_i = 0 - 3$  vibrational levels of the resonant

state.<sup>34</sup> Further details are given in ref. 34. Only the  $\Delta v = 0$  branches are shown. The rotational branching ratios are seen to be very dependent on the vibrational level accessed in the resonant state with a strong  $\Delta N = \text{odd}$  ( $\ell = \text{even}$ ) propensity rule evident in lower vibrational levels and a  $\Delta N = \text{even}$  ( $\ell = \text{odd}$ ) propensity rule for higher vibrational excitation. This vibrational state dependence of ionic rotational distributions is expected to occur in other diatomic hydrides.

● *Molecular alignment from photoelectron angular distributions:* Studies of molecular alignment – molecules with a preferred plane of rotation – are of increasing interest due to the detailed dynamical information these studies can provide on processes such as photofragmentation,<sup>35</sup> chemical reactions, and gas-surface scattering.<sup>36</sup> For example, photofragment alignment relates directly to stereochemical aspects of the dissociation process such as the plane of dissociation and torsional motion of the fragment before dissociation. In beam studies of inelastic scattering of molecules from surfaces, alignment probes the forces acting during the molecule-surface encounter.

Conventionally, fluorescence techniques are used to probe state alignment. When the state does not fluoresce itself, laser induced fluorescence (LIF) methods are used. On the other hand, angle-resolved  $(n + 1)$ -REMPI is not commonly used to probe state alignment. The bound-continuum nature of the ionization step, coupled with the anisotropy associated with photon absorption, causes state alignment information to be intimately entangled with the photoionization dynamics. Even angle-integrated cross sections from  $(n + 1)$ -REMPI spectra contain alignment information mixed in with the photoionization dynamics.

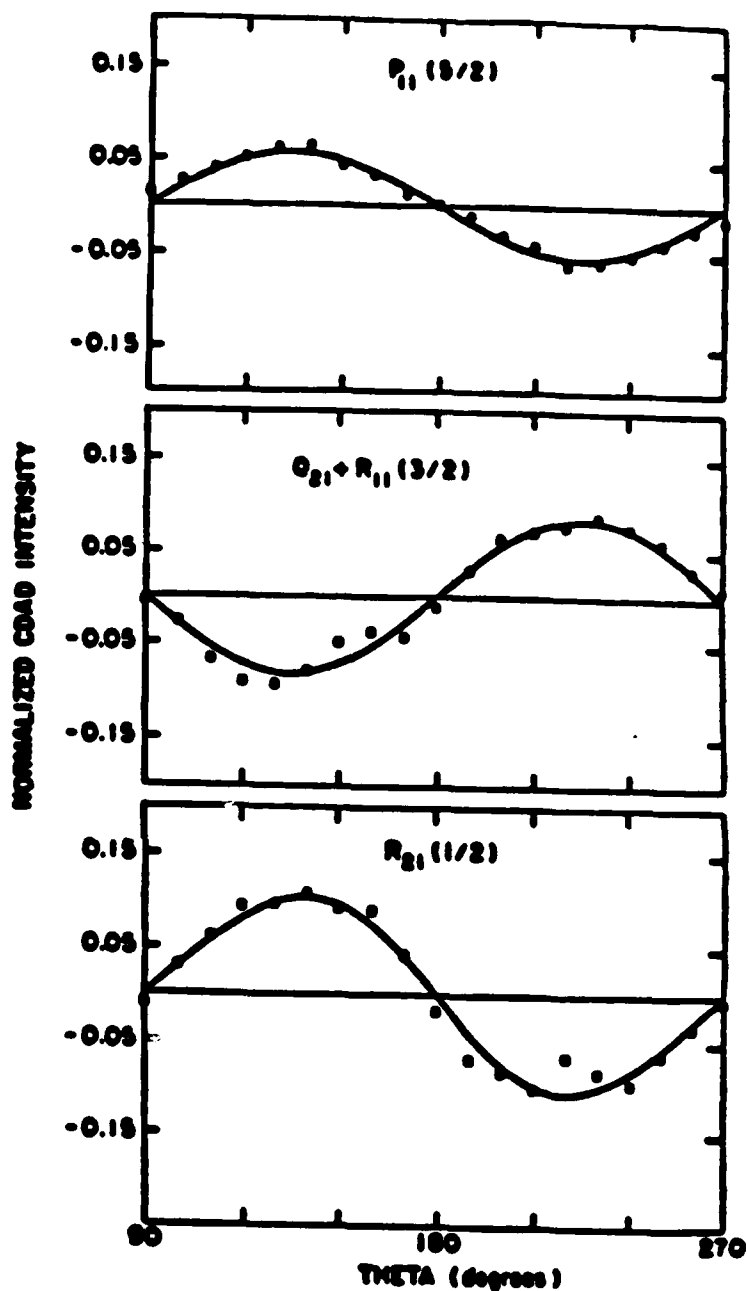
We have shown that the photoelectron angular distributions resulting from ionization of aligned linear molecules should exhibit a dichroic asymmetry, i.e., angular distributions from aligned states are different for photoionization with left- or right-circularly polarized light.<sup>13</sup> Circular dichroism is a phenomenon in which the response of a system to left- and right-circularly polarized light is different. *Circular dichroism or optical activity*

is normally associated with chiral molecules, i.e., molecules which have neither a plane nor center of symmetry, and not with linear molecules. A well-known manifestation of such dichroic behavior is molecular optical activity in the region of discrete absorption where the absorption coefficients for left- and right-circularly polarized light are different. In the region of continuous electronic absorption, i.e., photoionization, circular dichroism could be characterized by measurement of the angular distributions of photoelectrons produced by left- and right-circularly polarized light. Our prediction asserted that this circular dichroism in angular distributions (CDAD) – defined as the difference between angular distributions for photoionization with right- and left-circularly polarized light – occurs in linear molecules, arises in the electric dipole approximation (the leading term in the interaction between the molecule and the radiation), and would be a direct signature of the alignment of the molecule.<sup>13</sup> A question that immediately arises is: will these CDAD spectra be large enough to make their measurement feasible and practical? The answer will obviously be critical in determining whether CDAD has the potential of becoming a practical probe of molecular alignment. The question of the magnitude of the CDAD spectra (a difference spectra) is an important one since our theory showed that the effect arises from interference between different components, e.g.,  $\sigma$  and  $\pi$ , of the photoelectron orbital.<sup>10,11</sup>

To help establish the practicality of CDAD measurements we showed, by direct calculation, that CDAD spectra from optically aligned rotational levels of the  $A^2\Sigma^+$  state of  $NO$  should be about 15 – 25% of the “right” or “left” photoelectron spectra, suggesting that measurements were indeed currently possible.<sup>13</sup> Subsequently, in a joint experimental-theoretical study with M. G. White of Brookhaven National Laboratory, the CDAD spectra were measured for such optically aligned levels of  $NO$  and shown to be well described by the results of our calculations.<sup>14</sup> This work also demonstrated that CDAD spectra provide information about excited state alignment in both their phase and magnitude (see insert on next page). The phase relates to the shape of the  $M_J$  distribution and the magnitude



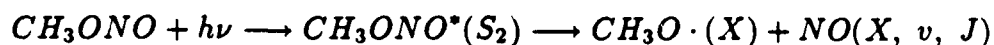
- Illustration of the dependence of the phase and magnitude of CDAD spectra on excited state alignment. These are CDAD spectra for three rotational transitions leading to the  $J' = 3/2$  level of the  $A^2\Sigma^+$  state of  $NO$ :  
 , experimental data of ref. 14  
 ; —, least squares fit to theoretically predicted functional form.



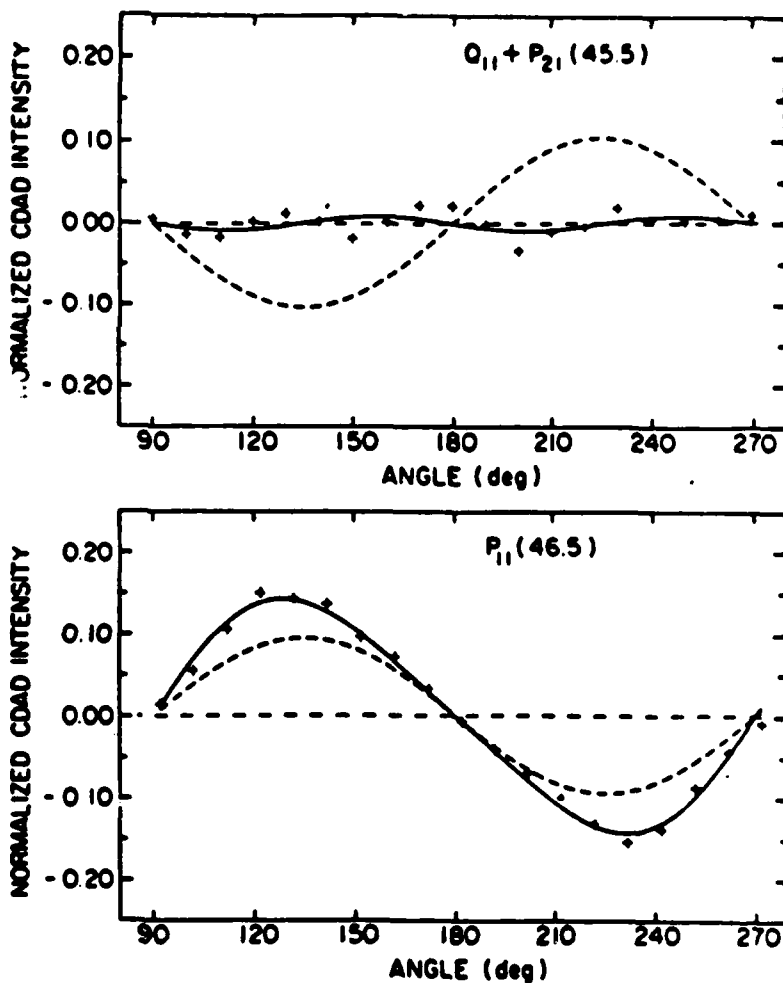
relates to the degree of alignment.

These studies served to establish a foundation for the extension of the CDAD technique to the significant application of determining ground state alignment induced by processes such as photofragmentation. We also showed that such *initial state alignment*, e.g., in a photofragment, can, in fact, be extracted from CDAD spectra in a straightforward manner, independently of the photoionization dynamics, by simply carrying out the

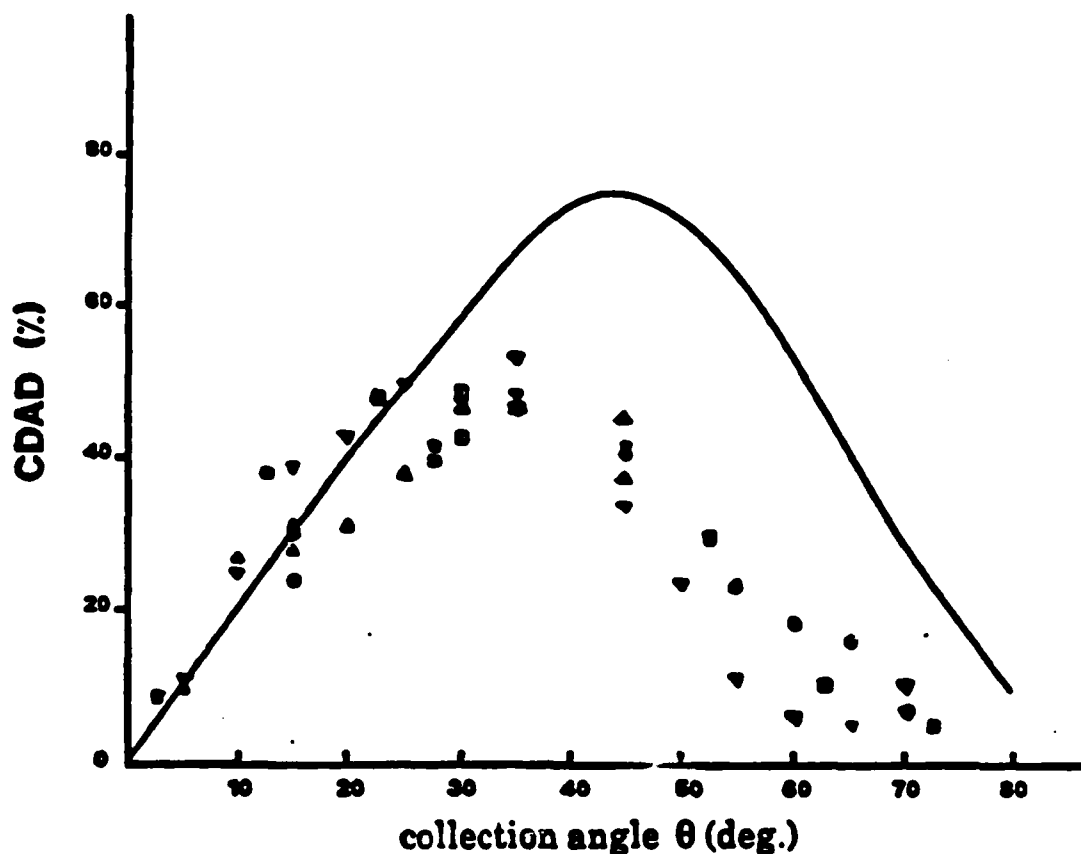
measurement via two different spectral branches.<sup>37</sup> This feature clearly removed one of the significant obstacles to practical use of the technique experimentally. In a further collaboration with M. G. White of the Brookhaven National Laboratory, the CDAD technique has been used for the first time to determine the spatial alignment of *NO* produced by UV photodissociation of methyl nitrite.<sup>15</sup>



- Illustration of the use of CDAD spectra to determine molecular alignment of a photofragment. The + are experimental data of ref. 15. The solid curves are best fits to the data using the theoretically predicted functional form. The dashed curves are for free (unaligned) *NO*. Details are given in ref. 15.



Some CDAD angular distributions from these studies are shown in the insert on page 25. These measurements have served to establish the utility of the CDAD method for probing chemical and physical processes in which spatial alignment plays an important role.<sup>15</sup>



- Circular dichroism in photoelectron angular distributions (CDAD) for  $CO$  ( $4\sigma$ ) on a Pd (111) surface at a photon energy of 33.3 eV: ▽ and ●, measurements of ref. 16; —, calculated CDAD spectra for a fixed isolated  $CO$  molecule modified to include the effect of free-electron-like refraction of the photoelectron by a surface potential barrier of 14 eV.

In an earlier and related development we had demonstrated that photoelectron angular distributions from linear molecules fixed in space,<sup>38</sup> e.g., adsorbed on surfaces, and from electronic orbitals (dangling) of surface atoms<sup>39</sup> should also exhibit a strong dichroic asymmetry. Such CDAD spectra could be a potentially useful probe of adsorbed molecules and surfaces. Tunable circularly polarized radiation at the photon energies

required for these studies is readily available at the BESSY synchrotron in Berlin. Recently measurements of the CDAD spectra for photoionization of the  $4\sigma$  level of  $CO$  adsorbed on a Pd (111) surface have been carried out at this facility.<sup>16,40</sup> These results (insert) show that the magnitude of this effect is large. Some measured CDAD spectra and those calculated for a "fixed"  $CO$  molecule (with refraction of the photoelectrons by a surface potential barrier) are shown in the insert. The CDAD effect was seen to reach values of up to 80% of the sum of the right and left spectra.<sup>16</sup> The technique is currently being exploited experimentally to study adsorbates and surfaces.<sup>16</sup>

## References

1. J. A. Stevens, M. Braunstein, and V. McKoy, *J. Chem. Phys.* **89**, 3923 (1988).
2. P. J. Miller, L. Li, W. A. Chupka, and S. D. Colson, *J. Chem. Phys.* **89**, 3921 (1988).
3. M. Braunstein, J. A. Stephens, and V. McKoy, **90**, 633 (1989).
4. J. A. Stephens, M. Braunstein, and V. McKoy, *J. Chem. Phys.* **92**, 5319 (1990).
5. S. N. Dixit, D. L. Lynch, V. McKoy, and A. U. Hazi, *Phys. Rev. A* **40**, 1700 (1989).
6. J. A. Stephens, M. Braunstein, D. L. Lynch, and V. McKoy, "Autoionization of repulsive valence states in (2+1) REMPI of  $O_2$  via the  $C^3\Pi_g$  Rydberg state," *J. Chem. Phys.* (manuscript in preparation).
7. W. A. Chupka, *J. Chem. Phys.* **87**, 1488 (1987).
8. A. P. Hickman, *Phys. Rev. Lett.* **59**, 1553 (1987).
9. J. A. Stephens and V. McKoy, *Phys. Rev. Lett.* **62**, 889 (1989).
10. K. Wang, J. A. Stephens, and V. McKoy, *J. Chem Phys.* **93**, 7863 (1990).
11. J. A. Stephens and V. McKoy, *J. Chem Phys.* **93**, 7863 (1990).
12. H. Rudolph, S. N. Dixit, V. McKoy, and W. M. Huo, *Chem. Phys. Letts.* **137**, 521 (1987).
13. R. L. Dubs, S. N. Dixit, and V. McKoy, *J. Chem. Phys.* **88**, 968 (1988).
14. J. R. Appling, M. G. White, R. L. Dubs, S. N. Dixit, and V. McKoy, *J. Chem. Phys.* **87**, 6927 (1987).
15. J. W. Winniczek, R. L. Dubs, J. R. Appling, V. McKoy, and M. G. White, *J. Chem. Phys.* **90**, 949 (1989).
16. G. Westphal, J. Bausmann, M. Getzlaff, G. Schönhense, N. Cherepkov, M. Braunstein, V. McKoy, and R. L. Dubs, *Surface Science* (1991).
17. See, for example, P. M. Dehmer, J. L. Dehmer, and S. T. Pratt, *Comments At. Mol. Phys.* **19**, 205 (1987).
18. P. J. Miller, L. Li, W. A. Chupka, and S. D. Colson, *J. Chem. Phys.* **89**, 3921

- (1988).
19. See, for example, J. L. Dehmer, D. Dill, and S. Wallace, *Phys. Rev. Lett.* **43**, 1005 (1979).
  20. P. J. Miller, W. A. Chupka, J. Winniczek, and M. G. White, *J. Chem. Phys.* **89**, 4058 (1988).
  21. P. J. Miller and W. A. Chupka (private communication).
  22. S. T. Pratt, P. M. Dehmer, and J. L. Dehmer, *Chem. Phys. Lett.* **105**, 28 (1984).
  23. S. N. Dixit, D. L. Lynch, and V. McKoy, *Phys. Rev. A* **30**, 3332 (1984).
  24. See, for example, H. Lefebvre-Brion and R. W. Field, *Perturbations in the Spectra of Diatomic Molecules* (Academic Press, Orlando, 1986), Chapter 4.
  25. W. G. Wilson, K. S. Viswanathan, E. Sakreta, and J. P. Reilly, *J. Phys. Chem.* **88**, 672 (1984).
  26. K. S. Viswanathan, E. Sekreta, E. R. Davidson, and J. P. Reilly, *J. Phys. Chem.* **90**, 5078 (1980).
  27. S. W. Allendorf, D. J. Leahy, D. C. Jacobs, and R. N. Zare, *J. Chem. Phys.* **91**, 2216 (1989).
  28. M. A. Sander, L. A. Chewter, K. Müller-Dethlefs, and E. W. Schlag, *Phys. Rev. A* **36**, 4543 (1987).
  29. S. N. Dixit and V. McKoy, *Chem. Phys. Lett* **128**, 49 (1986).
  30. H. Rudolph, S. N. Dixit, V. McKoy, and W. M. Huo, *J. Chem. Phys.* **88**, 637 (1988).
  31. S. N. Dixit, D. L. Lynch, V. McKoy, and W. M. Huo, *Phys. Rev. A* **32**, 1267 (1985).
  32. H. Rudolph, V. McKoy, and S. N. Dixit, *J. Chem. Phys.* **90**, 2570 (1989).
  33. H. Rudolph and V. McKoy, *J. Chem Phys.* **91**, 2235 (1989).
  34. H. Rudolph, J. A. Stephens, V. McKoy, and M.-T. Lee, *J. Chem. Phys.* **91**, 1374 (1989).

35. C. H. Greene and R. N. Zare, *Ann. Rev. Phys. Chem.* **33**, 119 (1982).
36. D. C. Jacobs, K. W. Kolasinski, R. J. Madix, and R. N. Zare, *J. Chem. Phys.* **87**, 5038 (1987).
37. R. L. Dubs, S. N. Dixit, and V. McKoy, *J. Chem Phys.* **86**, 5886 (1987).
38. R. L. Dubs, S. N. Dixit, and V. McKoy, *Phys. Rev. Letts* **54**, 1249 (1985).
39. R. L. Dubs, S. N. Dixit, and V. McKoy, *Phys. Rev. B* **32**, 8389 (1985).
40. C Westphal, J. Bausmann, M. Getzlaff, and G. Schönhense, *Phys. Rev. Lett.* **63**, 151 (1989).

● The research accomplishments outlined above have resulted in the following publications. The publications are listed in the sequence in which our major objectives are outlined in the Overview section of this report.

1. Shape-resonance-induced non-Franck-Condon effects in (2+1) resonance enhanced multiphoton ionization of the  $C^3\Pi_g$  state of  $O_2$   
J. A. Stephens, M. Braunstein, and V. McKoy  
*J. Chem. Phys.* **89**, 3923 (1988).
2. Shape resonance and non-Franck-Condon effects in (2+1)-REMPI of  $O_2$  via the  $C^3\Pi_g$  state  
M. Braunstein, J. A. Stephens, and V. McKoy  
*J. Chem. Phys.* **90**, 633 (1989).
3. Multiplet-specific shape resonance and autoionization effects in (2+1) resonance enhanced multiphoton ionization of  $O_2$  via the  $d^1\Pi_g$  state  
J. A. Stephens, M. Braunstein, and V. McKoy  
*J. Chem. Phys.* **92**, 2362 (1990).
4. Orbital evolution and promotion effects in the photoionization dynamics of  $^2\Sigma^-$  Rydberg states of OH  
J. A. Stephens, V. McKoy, S. N. Dixit, R. G. Tonkyn, and M. G. White  
*J. Chem. Phys.* **93**, 7863 (1990).
5. Non-Franck-Condon effects in photoionization of the  $3^3\Pi$  Rydberg state of NH  
K. Wang, J. A. Stephens, and V. McKoy  
*J. Chem. Phys.* **93**, 7874 (1990).
6. (2+1)-REMPI of NO via the  $D^2\Sigma^+$  state: rotational branching ratios  
H. Rudolph, S. N. Dixit, V. McKoy, and W. M. Huo  
*Chem. Phys. Lett.* **137**, 521 (1987).
7. Electronic autoionization and vibrational state distributions in resonant multiphoton ionization of  $H_2$   
S. N. Dixit, D. L. Lynch, B. V. McKoy, and A. H. Hazi  
*Phys. Rev. A* **40**, 1700 (1989).



8. Ionic rotational branching ratios for resonant enhanced multiphoton ionization of NO via the  $A^2\Sigma^+(3s\sigma)$  and  $D^2\Sigma^+(3p\sigma)$  states  
H. Rudolph, S. N. Dixit, V. McKoy, and W. M. Huo  
*J. Chem. Phys.* **88**, 637 (1988).
9. (1+1)-REMPI via the  $A^2\Sigma^+$  state of NO: ionic rotational branching ratios, and their intensity dependence  
H. Rudolph, S. N. Dixit, V. McKoy, and W. M. Huo  
*J. Chem. Phys.* **88** 1516 (1988).
10. Rotational branching ratios at low photoelectron energies in resonant enhanced multiphoton ionization of NO  
H. Rudolph, V. McKoy, and S. N. Dixit  
*J. Chem. Phys.* **90**, 2570 (1989).
11. Vibrational state dependence of ionic rotational branching ratios in resonance enhanced multiphoton ionization of CH  
H. Rudolph, J. A. Stephens, V. McKoy, and M.-T. Lee  
*J. Chem. Phys.* **91**, 1374 (1989).
12. Rotationally-resolved photoelectron angular distributions in resonance enhanced multiphoton ionization of NO  
H. Rudolph and V. McKoy  
*J. Chem. Phys.* **91**, 2235 (1989).
13. Dependence of NO rotational photoionization propensity rules on electron kinetic energy  
X. Song, E. Sekreta, J. P. Reilly, H. Rudolph, and V. McKoy  
*J. Chem. Phys.* **91**, 6062 (1989).
14. Cooper minima and rotationally resolved resonance enhanced multiphoton ionization spectroscopy  
H. Rudolph and V. McKoy  
*J. Chem. Phys.* **91**, 7995 (1989).

15. (2+1') Rotationally resolved resonance enhanced multiphoton ionization via the  $E^2\Sigma^+(4s, 3d)$  and  $H^2\Sigma^+(3d, 4s)$  Rydberg states of NO  
H. Rudolph and V. McKoy  
*J. Chem. Phys.* **93**, 7054 (1990).
16. Shape resonance effects in the rotationally resolved photoelectron spectra of  $O_2$   
M. Braunstein and V. McKoy  
*J. Chem. Phys.* **93**, 5345 (1990).
17. Atomic and molecular alignment from photoelectron angular distributions in (n+1)-resonantly enhanced multiphoton ionization  
R. L. Dubs, S. N. Dixit, and V. McKoy  
*J. Chem. Phys.* **88**, 968 (1988).
18. Molecular alignment from circular dichroic photoelectron angular distributions in (n+1) resonance enhanced multiphoton ionization  
R. L. Dubs and V. McKoy  
*J. Chem. Phys.* **91**, 5208 (1989).
19. (1+1) CDAD: a new technique for studying photofragment alignment  
R. L. Dubs, S. N. Dixit, and V. McKoy  
*J. Chem. Phys.* **86**, 5886 (1987).
20. Circular dichroism in photoelectron angular distributions from two-color (1+1')-REMPI of NO  
J. R. Appling, M. G. White, R. L. Dubs, S. N. Dixit and V. McKoy  
*J. Chem. Phys.* **87**, 6927 (1987).
21. A REMPI study of the photodissociation dynamics of the  $S_2$  state of  $CH_3ONO$   
J. W. Winniczek, R. L. Dubs, J. R. Appling, V. McKoy, and M. G. White  
*J. Chem. Phys.* **90**, 949 (1989).
22. Circular dichroism in photoemission from oriented molecules at surfaces  
C. Westphal, J. Bansmann, M. Getzlaff, G. Schönhense, N. A. Cherepkov, M. Braunstein, and V. McKoy  
*Surface Science* (accepted for publication).

● **The following invited papers were presented.**

23. **Some computational studies in molecular physics**

V. McKoy, R. L. Dubs, and S. N. Dixit

Invited lecture at the Conference on Grand Challenges to Computational Science held on Molokai, Hawaii, January 1989.

*Future Generation Computer Systems* **5**, 213 (1989).

24. **Photoelectron spectroscopy of excited molecular states**

V. McKoy, M. Braunstein, H. Rudolph, J. A. Stephens, S. N. Dixit, and D. L. Lynch

Invited lecture at the IV International Conference of Electron Spectroscopy held in Honolulu, Hawaii, 1989.

*J. Electron Spectroscopy and Related Phenomena* **52**, 597 (1990).

25. **Non-Franck-Condon effects induced by shape resonances and orbital evolution in resonance enhanced multiphoton ionization of small molecules**

J. Stephens, M. Braunstein, V. McKoy, H. Rudolph, and M.-T. Lee

Invited lecture at the Ninth International Conference on Vacuum Ultraviolet Radiation Physics held in Honolulu, Hawaii, July 17-21, 1989

*Physica Scripta* **41**, 482 (1990).

● **In addition to invited seminars at several institutions, the following invited presentations were also made.**

● **Rotational and Vibrational Distributions in Molecular REMPI**

Gordon Research Conference on Multiphoton Processes, June 11-15, 1990, New London, New Hampshire.

● **Rotational and Vibrational Ion Distributions in Resonance Enhanced Multiphoton Ionization of Molecules**

Symposium on Resonance Enhanced Multiphoton Ionization Processes in Atoms and Molecules

Spring Meeting of the American Physical Society, April 18-21, 1988, Baltimore, Maryland.

## ● Education, Training, and Professional Personnel

### ● Graduate Students Supported

1. Richard L. Dubs (1987-1988)
2. Matthew Braunstein (1987-1989)
3. Henrik Rudolph (1987-1989)

### ● Degrees Granted and Ph.D. Thesis Titles

1. Richard L. Dubs

Thesis title: *Single- and Multiphoton Ionization Processes in Molecules*  
(June, 1988)

2. Henrik Rudolph

Thesis title: *Dynamics of Rotationally Resolved Multiphoton Ionization Processes in Molecules* (June, 1989)

3. Matthew Braunstein

Thesis title: *Photoionization Dynamics and Ion State Distribution in Single-Photon and Resonance Enhanced Multiphoton Ionization of Molecules* (June, 1990)

### ● Postdoctoral Fellows

1. Jeffrey A. Stephens (1987-1990)
2. K. Wang (1988-1990)